Langmuir

ARTICLE

pubs.acs.org/Langmuir

Pseudopolyrotaxanes on Inorganic Nanoplatelets and their Supramolecular Hydrogels

Xiaojuan Liao, Guosong Chen,* and Ming Jiang*

Key Laboratory of Molecular Engineering of Polymers of Ministry of Education, Department of Macromolecular Science, Fudan University, Shanghai 200433, P. R. China

Supporting Information

ABSTRACT: In this paper, we demonstrate the first hybrid suprastructure of pseudopolyrotaxanes (PPRs) on clay nanoplatelets. Simple end-modification of poly(ethylene glycol) with pyridinium (PEG-$\mathbf{N}^+$) enabled the chains to form brushlike conformation on clay surfaces. Thus, the PEG chains were able to thread into the cavities of α-cyclodextrins (α-CDs), leading to hybrid PPR hydrogels. This was very different from the unmodified PEG chains, which were absorbed onto the clay surface and thus made the PPR formation impossible. The hydrogels made of this PPR-on-clay structure displayed a dynamic modulus 1 order of magnitude higher than those of the native PPR hydrogels. Furthermore, based on the competitive host−guest interactions, such hybrid hydrogels showed fully photoreversible sol−gel transition after a competitive guest containing azobenzene moiety was introduced.

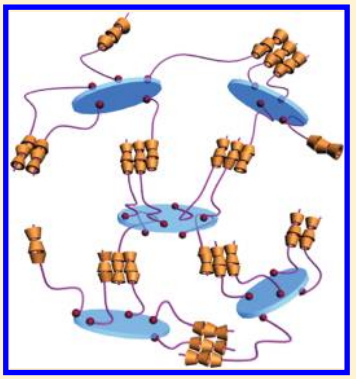

INTRODUCTION

Polymeric hydrogels have been extensively investigated for a few decades. In recent years, they have attracted ever-growing attention because they are essentially green soft materials composed of a large amount of water and small part of organic species.[1] One of the remarkable progresses in this field was the contribution of Haraguchi and Takehisa in introducing clay nanoplatelets into the synthetic polymeric hydrogels.[2] The mechanical properties were significantly improved as the clay served as a multifunctional cross-linker connecting the polymer chains. Furthermore, very recently, Aida et al. succeeded in preparing hybrid hydrogels from clay and telechelic dendritic macromolecules, where the latter bind to the former with multiple adhesive termini.[1a] The hydrogel was featured by great mechanical strength as well as rapid and complete self-healing behavior. These achievements have proved the very efficient role of clay in fabricating new polymeric hydrogels with outstanding properties. However, up to now, no reports on introducing clay nanoplatelets into pseudopolyrotaxane (PPR) hydrogels appeared, which were based on the supramolecular host−guest interactions. The most extensively studied PPR hydrogel is composed of guest polymers poly(ethylene glycol) (PEG) and host α-cyclodextrins (α-CDs), where the former as the axis thread into the cavities of the latter, and the threaded α-CDs form microcrystal domains, which serve as physical cross-linkers.[3] Since its first appearance in 1994, different kinds of guest polymers, including block copolymers, grafted polymers, and star-shape polymers, have been employed.[4] The PPR hydrogel is promising as a biomedical material because of its shear-thinning properties,[5] although it usually suffers from mechanical weakness.

Introducing clay nanoplatelets into PPR hydrogels is very attractive, as it may improve the mechanical properties and reduce the organic content. However, in practice, the strong interactions between PEG chains and clay, which have been reported,[6] make the chains adhere to the platelet surfaces, and thus the PEG chains threading into CD cavities becomes impossible. In this Article, we report a simple way of anchoring PEG chains to the clay surface via electrostatic interactions by capping the end of PEG with a pyridinium group (PEG-$\mathbf{N}^+$, Scheme 1). Thus, the chains are oriented away from the surface. Such PEG brushes are then able to thread into CDs and consequently form hybrid PPR hydrogels with improved mechanical properties. In addition, the PPR hydrogel can perform photoswitchable sol−gel transitions fully based on supramolecular principles.[7] Therefore, this work shows that the resultant clay-PPR hydrogels are more suitable candidates as potential biomedical materials.

EXPERIMENTAL SECTION

Materials. α-CD (TCI, GR), synthetic hectorite "Laponite XLG" (Rockwood Ltd.: $[Mg_{5.34}Li_{0.66}Si_8O_{20}(OH)_4]Na_{0.66}$, layer size = 20−30 nm $\Phi \times 1$ nm, cation exchange capacity =104 mequiv/100 g), poly(ethylene glycol) methyl ether (PEG, Aldrich, M_n = 5000), Pluronic copolymer (Aldrich, M_n = 14 600, PEO content 82.5%), and 2-bromoisobutyryl bromide (Aldrich, 97%) were commercially available. Benzoyl peroxide (BPO) was recrystallized twice from chloroform before use. *N*,

Received: July 6, 2011
Revised: August 24, 2011
Published: September 08, 2011

Scheme 1. Chemical Structures of PEG-N$^+$ and Azo-N$^+$

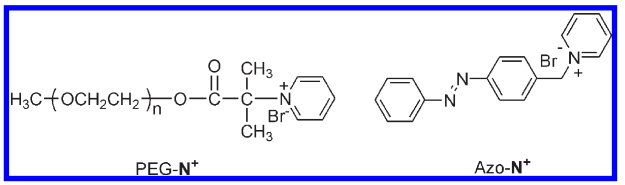

N-Dimethylformamide (DMF) was dried over calcium hydride and distilled under reduced pressure. Other general chemicals, including nitrosobenzene, *p*-aminotoluene, *N*-bromosuccinimide (NBS), pyridine, and so forth, were used as received.

Characterization Techniques. ^{1}H NMR spectra were recorded on a Bruker DMX500 instrument. UV−vis spectra were taken on a Perkin-Elmer Lambda 35 UV−vis spectrophotometer. Fourier transform infrared (FT-IR) spectra were recorded on a Nexus 470 FT-IR spectrometer using powder-pressed KBr pellets. Thermal gravimetric analysis (TGA) measurements were carried out on a Perkin-Elmer Pyris-1 series thermal analysis system under a flowing nitrogen atmosphere at a scan rate of 20 °C/min from 50 to 700 °C. X-ray diffraction (XRD) measurements were carried out on a PANalytical X'Pert Pro X-ray diffractometer with Cu Kα (1.542 Å) radiation (40 kV, 40 mA). The rheological behavior of the hydrogels was investigated via a Malvern rheometer using 40 mm parallel-plate geometry, cone-plate geometry, or cup-bob at 25 °C. Oscillating strain was fixed at 0.1% for all dynamic tests. Dynamic laser light scattering (DLS) experiments were carried out on an ALV/5000E instrument with the scattering angle of 90° at 25 ± 0.1 °C. R_h was calculated by cumulants simulation.

Synthesis of PEG-N$^+$ and Azo-N$^+$. To get PEG modified clay, PEG-N$^+$ was synthesized in two steps, which is shown in Scheme S1 in the Supporting Information.

Synthesis of PEG-Br. PEG (M_n = 5000, 5 g, 1 mmol) and triethylamine (0.84 mL, 6 mmol) were dissolved in dry $CHCl_3$ and kept at 0 °C, and then 2-bromoisobutyryl bromide (0.55 mL, 5 mmol) in dry $CHCl_3$ was added dropwise. Then the mixture was kept at room temperature for 48 h. The crude product was filtered, extracted, dried over anhydrous $MgSO_4$, precipitated by ethyl ether, and finally recrystallized in ethanol. The product was dried in vacuum overnight.

*Synthesis of PEG-**N**$^+$.* PEG-Br (5 g, 1 mmol) and pyridine (0.8 mL, 10 mmol) were dissolved in DMF (30 mL). The mixture was stirred at 100 °C for 48 h. After being cooled to room temperature, the mixture was concentrated, precipitated from petroleum ether, and recrystallized in ethanol. The product was dried under vacuum overnight. The ^{1}H NMR spectrum of PEG-N$^+$ in $CDCl_3$ is shown in Figure S1 in the Supporting Information. The functionalization degree of PEG is 95% estimated by ^{1}H NMR.

*Synthesis of Azo-**N**$^+$.* Azo-N$^+$ was synthesized as we described before.[7]

Preparation of Photoresponsive Hybrid Hydrogel. C-PEGN$^+$-PPR hydrogel was prepared as follows. First, clay was ion exchanged with PEG-N$^+$ in aqueous solution to get PEG-N$^+$ modified clay (named C-PEGN$^+$). Then an aqueous solution of α-CD was added, and the mixture was kept in the refrigerator at 4 °C overnight. The desired hybrid hydrogel was thus obtained. Photoreversibility of the hydrogel: an equivalent molar amount of *trans*-Azo-N$^+$ to α-CD in water was added into the hydrogel. After ultrasonication treatment, the gel turned into sol in a few minutes. Subsequent UV irradiation at 365 nm of the resultant sol made it return to hydrogel. This hydrogel went to sol again after visible light irradiation. Such gel-to-sol and sol-to-gel transitions were realized repeatedly as visible and UV irradiations were alternately performed.

Preparation of Native PPR and Pluronic PPR Hydrogel. Native PPR hydrogel was prepared according to the literature.[3c] An aqueous solution of α-CD was first mixed with PEG solution, followed by sonication and standing at 4 °C overnight, leading to the formation of native PPR hydrogel. Pluronic PPR hydrogel was prepared as that of native PPR hydrogel by using pluronic copolymer (triblock of PEO-*b*-PPO-*b*-PEO) instead of PEG.

RESULTS AND DISCUSSION

Differences in Chain Conformation between PEG and PEG-N$^+$ on Clay Surface. Pyridinium-ended PEG (PEG-N$^+$) was first designed and synthesized (Supporting Information, Scheme S1, Figure S1). The positively charged end-group pyridinium is the same as that in Azo-N$^+$ (1-[*p*-(phenylazo)-benzyl]pyridinium bromide, Scheme 1), which was used as a competitive guest in our previous work on reversible sol−gel transitions in PPR hydrogel composed of PEG and α-CDs.[7] PEG-N$^+$ and clay (synthetic hectorite "Laponite XLG") were mixed in water. After centrifugation, the obtained solid was washed with ethanol, which was a good solvent for PEG, leading to hybrid platelets due to the ion-exchange reaction. The platelets (C-PEGN$^+$) contained both clay and PEG-N$^+$ as shown in the infrared spectra (IR, Supporting Information, Figure S2).

From thermogravity analysis (TGA) of C-PEGN$^+$, PEG-N$^+$ and clay (Figure S3, Supporting Information), the PEG-N$^+$ content in the modified clay was estimated to 30%. In addition, the decomposition temperature of PEG-N$^+$ in the hybrid nanoplatelets is apparently higher than that of native PEG-N$^+$. The zeta-potential of the pure clay platelets in water was about −47.6 mV; with an addition of PEG-N$^+$ (80 wt % related to clay), the zeta-potential decreased to −30.8 mV, which could be attributed to the partial neutralization of the surface charge due to the interaction with PEG-N$^+$. However, addition of neutral PEG to clay (C-PEG) caused almost the same zeta-potential of −31.2 mV. This is reasonable as PEG can also be absorbed and coated on the clay surface, which has been deeply investigated by small-angle neutron scattering, light scattering, and rheology in diluted solution or hydrogel state.[6] Although IR, TGA and zeta-potential measurements provide important basic data for the hybrid nanoplatelets, they cannot tell the possible difference in conformational features between the PEG chains in C-PEGN$^+$ and C-PEG, which causes very different behavior in constructing PPR hydrogels as will be discussed below.

NMR studies provide more information. As shown in Figure S4 in the Supporting Information, the proton peak of PEG-N$^+$ dissolved in water as free chains was very sharp with an integration value 345, where the protons of the end group OCH_3 were used as a reference. After mixing PEG-N$^+$ with clay (C-PEGN$^+$), the integration of the peak decreased to 230, indicating that the mobility of PEG-N$^+$ chains here was less than that of the free chains. However, for the mixture of the neutral PEG and clay (C-PEG), at the same experimental condition, a much broader peak appeared with a smaller integration value of 205. As reported in the literature,[6] PEG chains strongly interact with clay and then attach to and coat on the clay surface. Thus, the NMR results of C-PEG showing highly restricted mobility of the chains are in agreement with this model. However, in C-PEGN$^+$, both broadness and height of the proton peak are between those of the free chains and the neutral PEG chains on the surface. This indicates that the PEG-N$^+$ chains on the clay surface display relatively extended conformation with a larger chain mobility in solution, different from that of the neutral PEG chains lying on the clay surface.

dx.doi.org/10.1021/la202555t |*Langmuir* 2011, 27, 12650–12656

Table 1. DLS Results of Clay, C-PEG, C-PEGN$^+$, C-PEG-α-CD, and C-PEGN$^+$-PPR

	clay	C-PEG	C-PEGN$^+$	C-PEG-α-CD	C-PEGN$^+$-PPR
R_h (nm)[a]	17.1	17.5	19.5	17.9	24.1
SI[b]	96.9	230	287	229	544

[a] Hydrodynamic radius. [b] Relative scattering intensity.

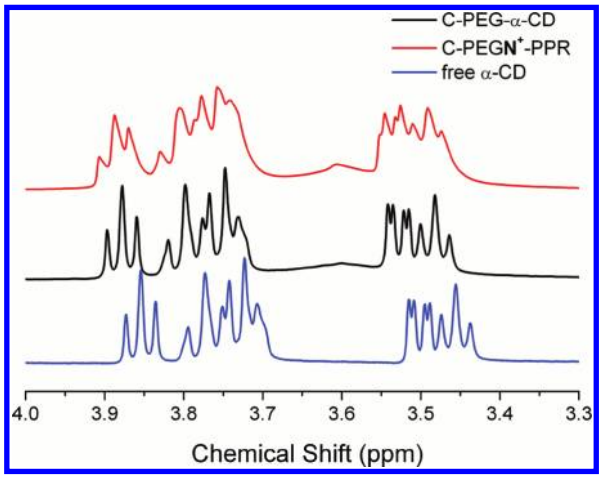

Figure 1. ^{1}H NMR spectra of free α-CD (blue), C-PEG-α-CD (black), and C-PEGN$^+$-PPR (red) in D_2O.

To investigate the difference of the PEG and PEG-N$^+$ chains on the clay surface in detail, dynamic laser light scattering (DLS) measurements were conducted. As shown in Table 1 for the dilute solutions (concentrations: clay 4 mg/mL and PEG 3.2 mg/mL), as the scattered light intensity is roughly proportional to the "molecular weight" of the analyte,[8] the apparent intensity increase of C-PEG compared to that of the pure clay can be attributed to PEG adhering to clay. However, C-PEG showed the same R_h value as that of the pure clay, implying that the PEG layer on the clay platelets was very thin and the chains did not extend into solution as they were tightly absorbed. That was in accordance with the model in literature.[6] Interestingly, PEG-N$^+$ led to different results; that is, C-PEGN$^+$ showed an even larger scattered light intensity as well as a substantial size increase. This could be attributed to the more extended conformation of the PEG-N$^+$ chains with charged ends attaching to clay surface. As a result, C-PEG and C-PEGN$^+$ would show very different abilities as guests in inclusion complexation. When α-CD of the same amount as PEG was added into the C-PEG solution (C-PEG-α-CD), neither R_h nor the scattered light intensity changed, which meant that no inclusion complexation took place. It is reasonable that the PEG chains are not able to thread into the α-CD cavities as they have been immobilized onto the clay surface. In contrast, an addition of α-CDs into the C-PEGN$^+$ solution made obvious increases of the size from 19.5 to 24.1 nm and the relative scattered light intensity from 287 to 544. This could be attributed to the extended chains of PEG-N$^+$ threading into α-CD cavities. Therefore, by using the cation-ended PEG, pseudopolyrotaxanes of α-CDs and PEG on the clay nanoplatelets were successfully prepared, which was coded as C-PEGN$^+$-PPR. ^{1}H NMR results supported this conclusion. As shown in Figure 1, the α-CD part of C-PEG-α-CD spectrum (black) was the same as that of free α-CDs (blue), indicating the free state of α-CDs in its mixture with C-PEG. However, much broader peaks of α-CDs appeared in the spectrum of C-PEGN$^+$-PPR (red), compared with that in C-PEG-α-CD. This indicated that the mobility of α-CD was restricted by PEG-N$^+$ as a result of the formation of PEG-N$^+$-PPR and its further aggregation.

Scheme 2. Structural models of C-PEG (A), C-PEGN$^+$ (B), and C-PEGN$^+$-PPR (C)[a]

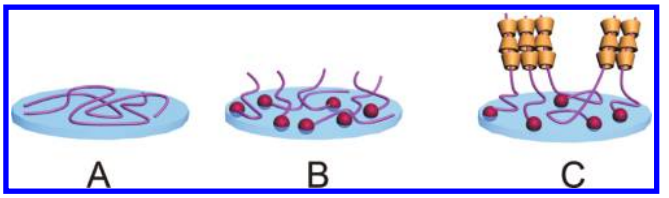

[a] For clarity, polymer chains on one side of clay are shown only, the same in the schemes below (blue plate, clay platelet; purple chain, PEG; purple chain with red head, PEG-N$^+$; yellow cavity, α-CDs).

Hybrid Platelets and Their Properties. Now based on all the results discussed above, we propose structural models for the hybrid platelets of C-PEG, C-PEGN$^+$ and C-PEGN$^+$-PPR (Scheme 2).

Model A is the same as that reported in the literature for the hybrid platelets containing neutral PEG.[6] One may wonder why such a small modification of PEG, that is, capping with a positively charged group, would cause such remarkable difference in chain conformation on the platelets. In order to explore this problem, we compared the mixing enthalpies of the pyridium group/clay and $-CH_2CH_2O-$ unit/clay by isothermal titration calorimetry (ITC, Supporting Information, Figure S5). ITC results show that the mixing enthalpy of the pyridinium groups with excess clay is 10.1 kcal/mol, about 10 times higher than that of CH_2CH_2O unit with clay. So it is reasonable to think that when PEG-N$^+$ is mixed with clay platelets, compared to the CH_2CH_2O units, the pyridinium ends would interact with the clay surface preferentially. In other words, the chain ends would occupy many interaction sites, enabling the chains to be "planted" on the clay surface. Therefore, the possible absorption of the PEG units on the surface could be significantly prevented. It is necessary to mention that in this measurement of mixing enthalpy of the pyridinium group with clay, Azo-N$^+$ was used to replace PEG-N$^+$. It was because that the molar ratio of pyridinium vs $-CH_2CH_2O-$ units in PEG-N$^+$ was very low so it was hard to differentiate the contributions of PEG and pyridinium to the measured heat release. In our typical case of PEG-N$^+$/clay (weight ratio 3/7), from the density and size of the clay platelets, it could be estimated that each platelet possesses about 52 chains and each PEG-N$^+$ chain occupies 20 nm^2 surface on average (details in the Supporting Information). Considering that the chain areas of PEG (M_w = 5000) with mushroom structure and the cross section of fully extended conformation are around 118 and 1 nm^2,[9] respectively, and for a typical PEG brush (M_w = 35000) on a gold plate, each chain occupies about 3.3 nm^2 (Supporting Information),[10] it could be concluded that in the present case, the PEG-N$^+$ chains would display a loose brush structure (model B). Here the PEG chains are extending to some degree and not tightly close to each other, which benefits further threading of PEG chains into α-CD cavities to form PPRs on clay nanoplatelets (Model C).

Such a significant difference in chain structures between C-PEG and C-PEGN$^+$ is reflected in their rheological properties.

dx.doi.org/10.1021/la202555t |Langmuir 2011, 27, 12650–12656

Typically, the viscosity of clay aqueous solution (concentration 29 mg/mL) was about 0.7 Pa·s, and it decreased to 0.1 Pa·s when PEG (80 wt % related to clay) was added, due to the shielding of the electric interactions between the clay platelets by the PEG layer, which was consistent with the literature.[11] However, a dramatic viscosity increase to 240 Pa·s was observed when PEG-N^+ was mixed with clay at the same conditions as that for the neutral PEG. Figure 2 shows the viscosity dependence of C-PEGN^+ on PEG-N^+ concentration. The viscosity was as low as the pure clay (0.7 Pa·s) when the concentration of PEG-N^+ was lower than 15 mg/mL, but it sharply increased to 240 Pa·s when the concentration reached 22 mg/mL. Such a dramatic viscosity increase in a very narrow concentration range is indicative of some network formation, as the PEG brushes are able to contact each other and form interplatelet chain entanglement. Such a loose and local network would be sensitive to shearing. Figure 3 displays a strong shearing effect on the viscosity of C-PEGN^+ platelets as a result of dissociation of the chain entanglement under the shear force. On the contrary, C-PEG platelets with low viscosity do not show such effect (Figure 3 inset).

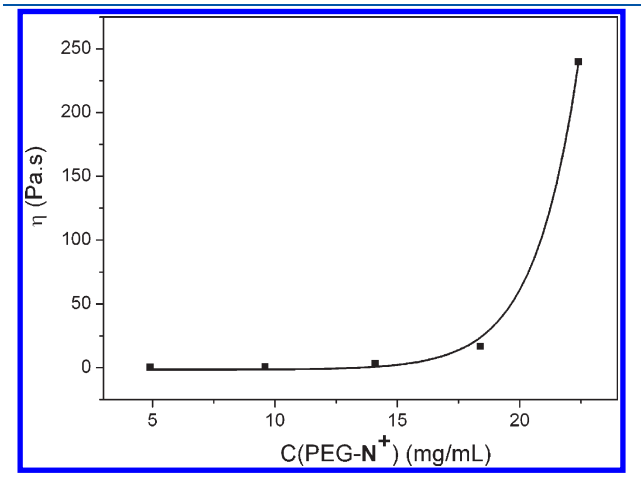

Figure 2. Viscosity of C-PEGN^+ aqueous solution as a function of concentration of PEG-N^+ (clay concentration is 29 mg/mL).

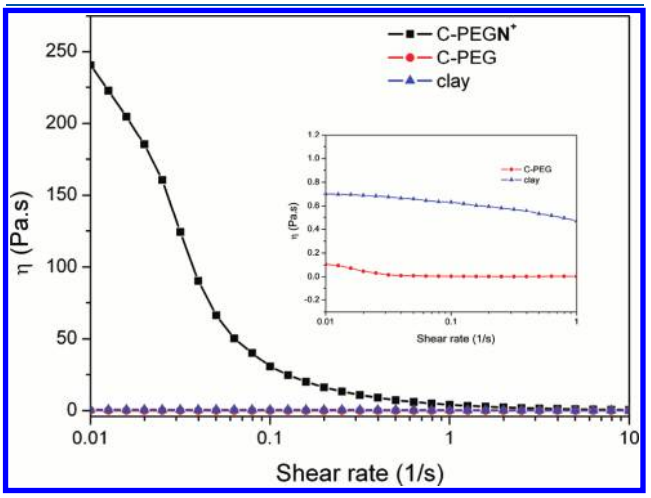

Figure 3. Steady rheological behavior of clay, C-PEG, C-PEGN^+ in aqueous solution. The inset is for clay and C-PEG with magnified ordinate. Concentrations of clay, PEG or PEG-N^+ were 29 and 22 mg/mL, respectively.

Hybrid PPR Hydrogels and Their Mechanical Properties. Furthermore, a hybrid PPR hydrogel was successfully prepared by mixing clay and PEG-N^+ at appropriate concentrations, that is, 18 mg/mL (clay), 14 mg/mL (PEG-N^+), and 55 mg/mL (α-CD). Figure 4 compares the elastic and viscous moduli of four different combinations with a common host of α-CD and different guest molecules, that is, neutral PEG, pluronic polymer (block copolymer of PEO-*b*-PPO-*b*-PEO), C-PEG, and C-PEGN^+. The corresponding structures of the PPR hydrogels are shown in Scheme 3. The preparation method was described in the Experimental Section. For these four samples, concentrations of PEG and α-CD were all the same. As an example for reference, the elastic modulus G' of the pluronic hydrogel was about 230 Pa, twice that of the native one, which was attributed to the hydrophobic aggregation of the PPO blocks. The most remarkable feature in Figure 4 is that both the elastic and viscous moduli of C-PEGN^+ hydrogel are the highest. Specifically, the elastic modulus G' of the C-PEGN^+ hydrogel is about 2.2 kPa, 1 order of magnitude higher than that of the native and pluronic hydrogels. This clearly shows the positive effect of introducing clay as an inorganic multifunctional cross-linker, which may enable the hydrogel to be applied as scaffold since many biological tissues have moduli in the range of kPa.[12] This result is also quite different from the hybrid PPR hydrogels with carbon nanotubes[13] and graphene[14] as inorganic cross-linkers where the moduli were smaller than those of the corresponding

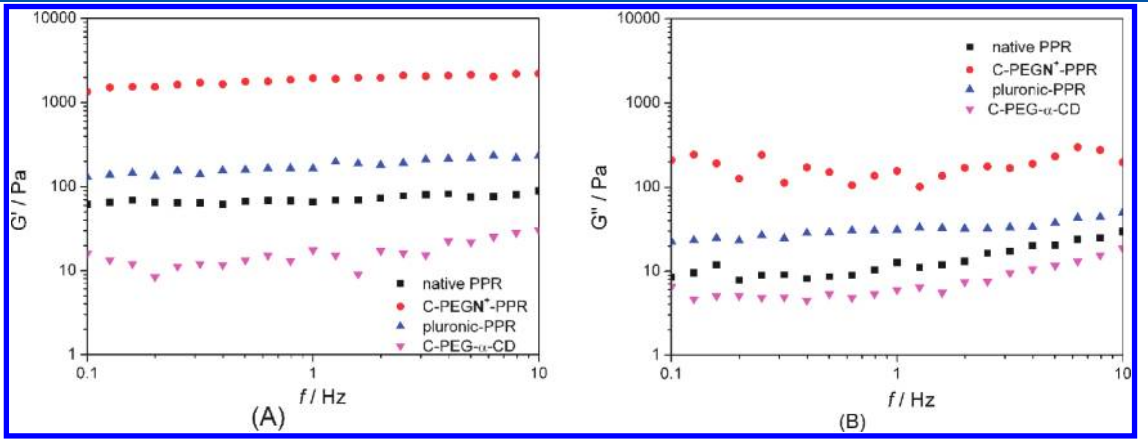

Figure 4. G' (A) and G'' (B) of hydrogels from native PPR, pluronic-PPR, C-PEGN^+-PPR, and C-PEG-α-CD.

dx.doi.org/10.1021/la202555t |*Langmuir* 2011, 27, 12650–12656

Scheme 3. Schematic Illustration of Different PPR Structures

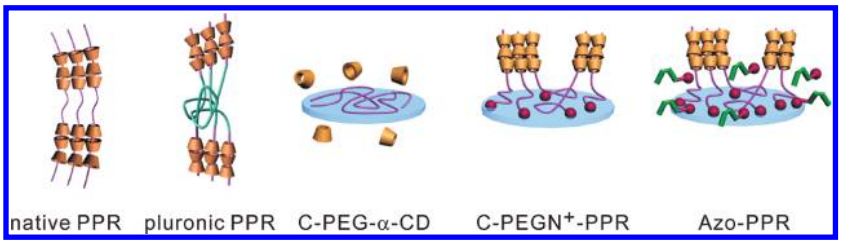

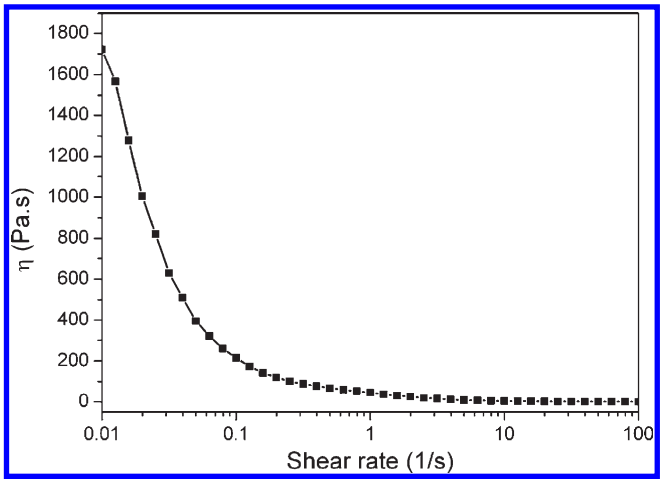

Figure 5. Steady viscosity of C-PEGN$^+$-PPR hydrogel as a function of shear rate.

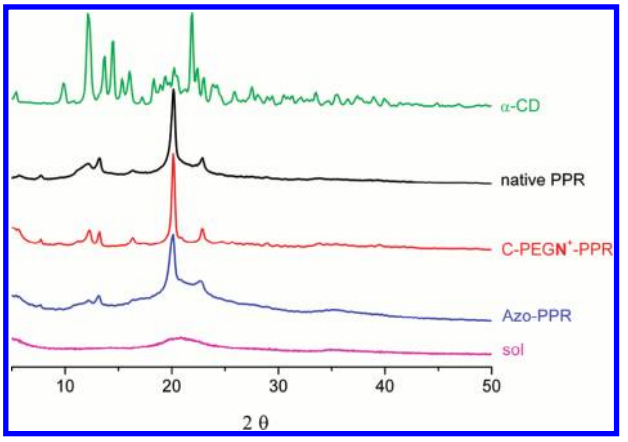

Figure 6. XRD patterns of (a) α-CD, (b) native PPR hydrogel of PEG/α-CD, (c) C-PEGN$^+$-PPR hydrogel, (d) Azo-PPR hydrogel, and (e) the corresponding sol of (d).

Scheme 4. Schematic Illustration of the C-PEGN$^+$-PPR Hydrogel

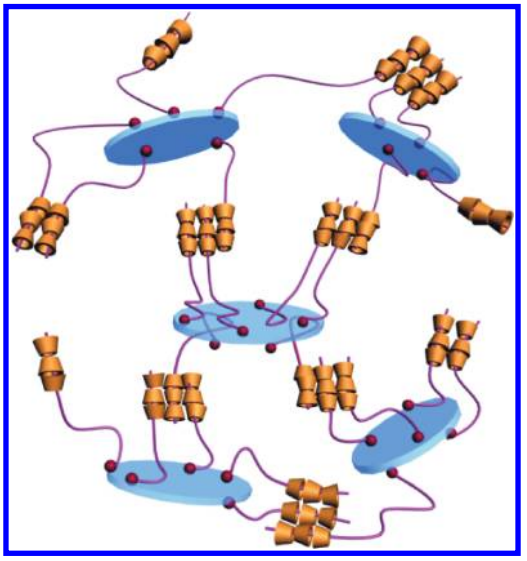

pluronic hydrogels. However, for C-PEG and α-CD, where the neutral PEG was used as a guest, G' was about 18 Pa, only one-fifth of the native hydrogel. This implies that the mixture of C-PEG and α-CD is not a real hybrid hydrogel. In short, from the rheological measurements, the significant role of the small modification of PEG in constructing the hybrid hydrogels was observed. In addition, the influence of feed ratio of different components on rheology behavior was studied in detail (Supporting Information, Figures S6−S8).

The PPR hydrogels made of PEG and α-CD are featured by their well-known shear-thinning properties, which are the base for their potential applications in nanomedicine.[5d,e] As shown in Figure 5, the hybrid hydrogel based on C-PEGN$^+$-PPR keeps this character. Viscosity dropped from 1700 to 68 Pa·s as the shear rate reached 0.5 s^{-1}. This indicates that the presence of clay has no effect on the shear thinning property which is caused by destroying the microcrystal domains composed of α-CD under shearing.

The C-PEGN$^+$-PPR hydrogel shows much higher viscosity and dynamic modulus than that of the native one as it contains two cross-link factors, as shown in Scheme 4. The first is the new multifunctional cross-linker, that is, the homogeneously incorporated clay nanoplatelets, which connect the PPR chains via ionic interactions. The second is the microcrystal domains formed by the threaded α-CDs. Wide angle X-ray scattering (WAXS) results of freeze-dried hydrogels of C-PEGN$^+$-PPR (Figure 6c) and native hydrogel of PEG/α-CD (Figure 6b) show the same pattern with the characteristic peak at 2θ = 20.1°, attributed to the channel-type structure of the α-CD and PEG complex.[15]

Photoreversibility of the Hybrid PPR Hydrogel. Recently, we reported that, for supramolecular hydrogels composed of PEG and α-CD, reversible sol−gel transition can be realized based on host−guest competitions by repeating UV and visible light irradiations.[7] The same principle was successfully employed in the current hybrid hydrogels of C-PEGN$^+$-PPR. For this

purpose, the azobenzene derivative Azo-N^+ with pyridinium group was used as a competitive guest for the inclusion complexation between PEG-N^+ and α-CD. When Azo-N^+ in water (an equivalent molar amount to α-CD) was added into the hydrogel of C-PEGN^+-PPR and the mixture was ultrasonicated, the hydrogel turned into sol in a few minutes. This is because the Azo-N^+ in *trans* form had much stronger interaction with α-CD than that between α-CD and PEG, thus α-CD was pulled off from the PEG chains leading to the dissociation of the hydrogel. It is noteworthy that the pyridinium group of Azo-N^+ had strong ionic interaction with clay as well (Figure S5, Supporting Information), so when it was mixed with the hydrogel, Azo-N^+ would adhere to clay surface. However, this fast gel-to-sol transition indicated that fixing of the pyridinium groups did not affect the inclusion complexation of the azobenzene species with α-CD. Subsequent UV irradiation at 365 nm on the resultant sol made it return to hydrogel (Figure 7). This indicated that *trans*-Azo-N^+ isomerized to its *cis* form under the irradiation, losing its ability to form an inclusion complex with α-CD, and thus, α-CD rings turned

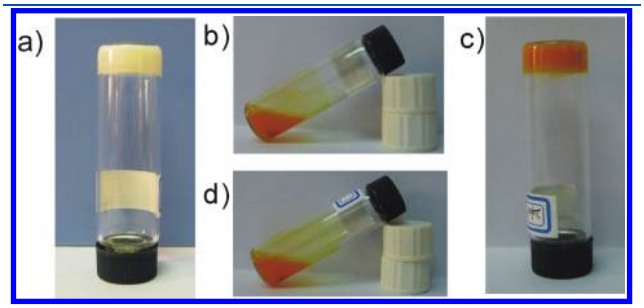

Figure 7. Hydrogels and corresponding sols: (a) C-PEGN^+-PPR hydrogel, (b) C/PEGN^+/α-CD/Azo-N^+ sol, (c) sol of (b) after UV irradiation, and (d) gel of (c) after visible-light irradiation.

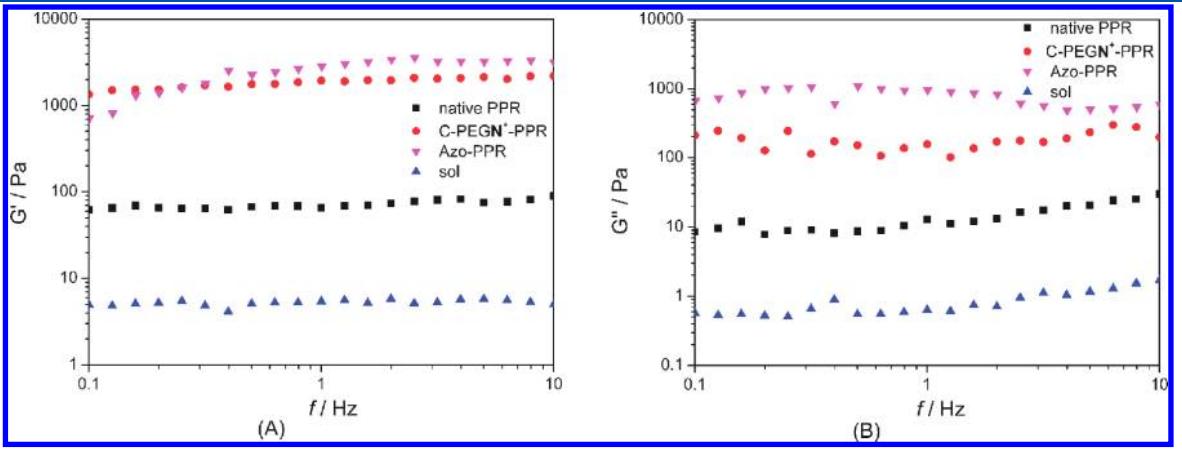

Figure 8. G' (A) and G'' (B) of native PPR, C-PEGN^+-PPR, sol, and Azo-PPR.

Scheme 5. Schematic Illustration for the Main Conclusions

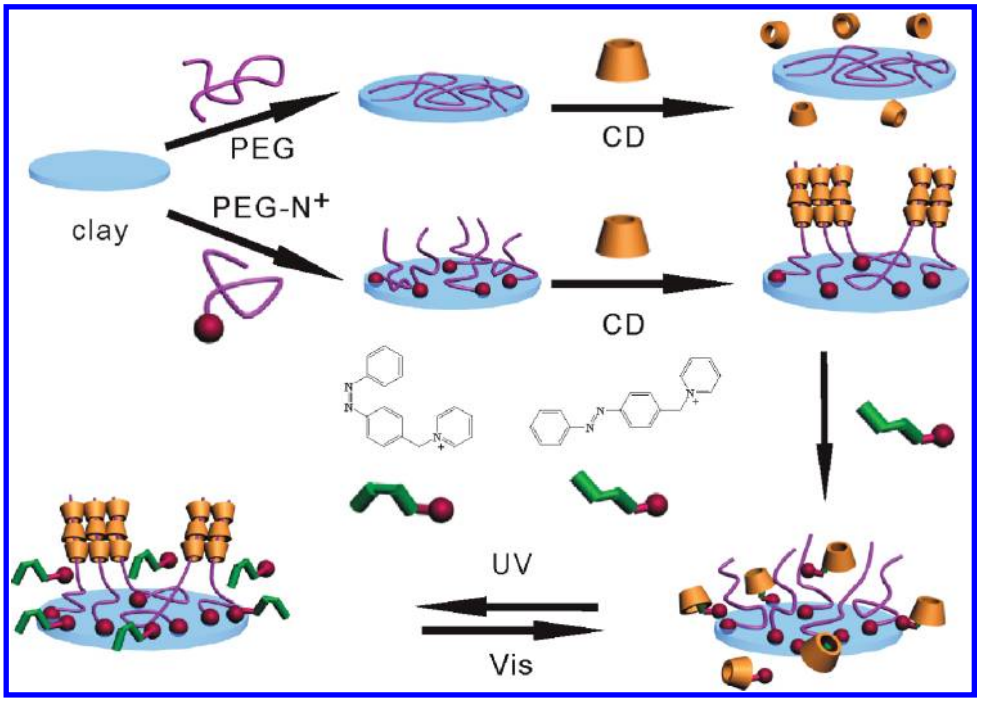

dx.doi.org/10.1021/la202555t |*Langmuir* 2011, 27, 12650–12656

back to be threaded by PEG chains, leading to the formation of hydrogel again. Such a regenerated hydrogel is simply noted as Azo-PPR (Scheme 3). Afterward, Azo-PPR hydrogel was irradiated by visible irradiation (435 nm) for 20 min; dissociation of the hydrogel took place as a result of *cis*-to-*trans* isomerization of Azo-N^+.

Figure 8 showed elastic and viscous moduli of the hydrogels from C-PEG$\mathbf{N}^+$-PPR and Azo-PPR. The recovered hydrogel Azo-PPR showed almost the same dynamic rheology properties (G' and G'') as the original hydrogel of C-PEG$\mathbf{N}^+$-PPR, and both were about 1 order of magnitude higher than that of the native PPR hydrogel. Furthermore, they had similar WAXS patterns (Figure 6) indicating the same microcrystal structures. However, the characteristic peak at $2\theta = 20.1°$ of Azo-PPR was not as sharp as that in C-PEG$\mathbf{N}^+$-PPR, which might be caused by the presence of the azobenzene groups onto the surface of clay, affecting the perfectness of the microcrystals. Both G' and G'' of the sol were very small, less than 10 Pa, and the characteristic peak at $2\theta = 20.1°$ disappeared completely in its WAXS pattern, indicating that there was no channel-type structure of α-CD and PEG complex.

CONCLUSIONS

Clay nanoplatelets were proven effective in improving mechanical properties of polymeric hydrogels in which the platelets played a role of hard multifunctional cross-linkers. However, for supramolecular PPR hydrogels composed of PEG and α-CD, simply introducing clay failed because PEG chains interacted with clay and laid on the clay surface so that the PEG chains were unable to form inclusion complexes with α-CDs. This work demonstrated that a simple modification of PEG, that is, capping the chain with pyridinium (PEG-$\mathbf{N}^+$), could make the chains form a brushlike conformation on the clay surface (Scheme 5). Such chains are able to thread into series of α-CD cavities, resulting in hybrid hydrogels. These hydrogels with homogeneously dispersed clay nanoplatelets display a dynamic modulus 1 order of magnitude higher than those of the native hydrogel of PEG and α-CD. Furthermore, such a hybrid hydrogel is active in supramolecular chemistry: by adding a competitive guest of Azo-N^+, the hydrogel dissociates due to the stronger interaction of *trans*-azobenzene than PEG with α-CD. Following alternating UV and visible light irradiation will make reversible sol-to-gel and gel-to-sol transitions due to the photoinduced isomerization of the azobenzene group (Scheme 5).

ASSOCIATED CONTENT

Supporting Information. Additional experimental details. This material is available free of charge via the Internet at http://pubs.acs.org.

AUTHOR INFORMATION

Corresponding Author

*Telephone: +86-21-65643919. Fax: +86-21-65643919. E-mail: mjiang@fudan.edu.cn (M.J.); guosong@fudan.edu.cn (G.C.).

ACKNOWLEDGMENT

Financial support from National Natural Science Foundation of China (No. 20834004 and 20904005) and Ministry of Science and Technology of China (2009CB930402 and 2011CB932503) are greatly acknowledged. We also thank Prof. K. Haraguchi for the generous gift of Laponite XLG.

REFERENCES

(1) (a) Wang, Q.; Mynar, J. L.; Yoshida, M.; Lee, E.; Lee, M.; Okuro, K.; Kinbara, K.; Aida, T. *Nature* **2010**, *463*, 339. (b) Gong, J. P. *Soft Matter* **2010**, *6*, 2583. (c) Tanaka, Y.; Gong, J. P.; Osada, Y. *Prog. Polym. Sci.* **2005**, *30*, 1.

(2) (a) Haraguchi, K.; Takehisa, T. *Adv. Mater.* **2002**, *14*, 1120. (b) Haraguchi, K. *Curr. Opin. Solid State Mater. Sci.* **2007**, *11*, 47.

(3) (a) Harada, A.; Kamachi, M. *Macromolecules* **1990**, *23*, 2821. (b) Harada, A.; Li, J.; Kamachi, M. *Nature* **1992**, *356*, 325. (c) Li, J.; Harada, A.; Kamachi, M. *Polym. J.* **1994**, *26*, 1019. (d) Harada, A.; Li, J.; Kamachi, M. *Nature* **1994**, *370*, 126.

(4) (a) Huh, K. M.; Ooya, T.; Lee, W. K.; Sasaki, S.; Kwon, I. C.; Jeong, S. Y.; Yui, N. *Macromolecules* **2001**, *34*, 8657. (b) He, L.; Huang, J.; Chen, Y.; Xu, X.; Liu, L. *Macromolecules* **2005**, *38*, 3845. (c) Yu, H.; Feng, Z.; Zhang, A.; Sun, L.; Qian, L. *Soft Matter* **2006**, *2*, 343.

(5) (a) Araki, J.; Ito, K. *Soft Matter* **2007**, *3*, 1456. (b) Guo, M. Y.; Jiang, M. *Prog. Chem.* **2007**, *19*, 557. (c) Li, J. *Adv. Polym. Sci.* **2009**, *222*, 79. (d) Li, J.; Ni, X. P.; Leong, K. W. *J. Biomed. Mater. Res., Part A* **2003**, *65*, 196. (e) Ni, X. P.; Cheng, A.; Li, J. *J. Biomed. Mater. Res., Part A* **2009**, *88*, 1031.

(6) (a) Loizou, E.; Butler, P.; Porcar, L.; Schmidt, G. *Macromolecules* **2006**, *39*, 1614. (b) Nelson, A.; Cosgrove, T. *Langmuir* **2004**, *20*, 2298. (c) Mongondry, P.; Nicolai, T.; Tassin, J.-F. *J. Colloid Interface Sci.* **2004**, *275*, 191.

(7) Liao, X. J.; Chen, G. S.; Liu, X. X.; Chen, W. X.; Chen, F. E.; Jiang, M. *Angew. Chem., Int. Ed.* **2010**, *49*, 4409.

(8) Dou, H. J.; Jiang, M.; Peng, H. S.; Chen, D. Y.; Hong, Y. *Angew. Chem., Int. Ed.* **2003**, *42*, 1516.

(9) (a) Du, H.; Chandaroy, P.; Hui, S. W. *Biochim. Biophys. Acta* **1997**, *1326*, 236. (b) Elli, S.; Eusebio, L.; Gronchi, P.; Ganazzoli, F.; Goisis, M. *Langmuir* **2010**, *26*, 15814.

(10) Dutta, A. K.; Belfort, G. *Langmuir* **2007**, *23*, 3088.

(11) Haraguchi, K.; Li, H. J.; Matsuda, K.; Takehisa, T.; Elliot, E. *Macromolecules* **2005**, *38*, 3482.

(12) (a) Aamer, K. A.; Sardinha, H.; Bhatia, S. R.; Tew, G. N. *Biomaterials* **2004**, *25*, 1087. (b) Hutmacher, D. W. *J. Biomater. Sci., Polym. Ed.* **2001**, *12*, 107.

(13) Wang, Z. M.; Chen, Y. M. *Macromolecules* **2007**, *40*, 3402.

(14) Zu, S. Z.; Han, B. H. *J. Phys. Chem. C* **2009**, *113*, 13651.

(15) Li, J.; Li, X.; Zhou, Z.; Ni, X.; Leong, K. W. *Macromolecules* **2001**, *34*, 7236.